Silicon (2018) 10:2547–2553
https://doi.org/10.1007/s12633-018-9789-0

ORIGINAL PAPER

Effect of Temperature on Electro-Optical Characteristics of Silicon Based p-n Photodiode (VTB8440BH)

Pradip Dalapati[1,2] · **Nabin Baran Manik**[1] · **Asok Nath Basu**[1]

Received: 10 June 2015 / Accepted: 28 February 2018 / Published online: 16 April 2018

Abstract
To get useful information about the carrier transport mechanism we first measure the current-voltage (I-V) characteristics of a silicon p-n photodiode (VTB8440BH) in the temperature range 350−110 K. All semilog I-V curves exhibit three successive linearly dependent regions along with their bias levels which are defined as I, II and III regions, respectively. Regions I and II with different slopes are used to determine the bias dependent ideality factors namely, n_1 and n_2. The variation of n_1 and n_2 with temperature shows that with lowering of temperature the tunneling probability gradually increases. Furthermore, these results are used to identify the paramount carrier at different bias levels. Secondly, to acquire knowledge of electron-hole generation rate we measure the variation of photocurrent in the same temperature range. Results show that photocurrent decreases slowly as temperature decreases from 350 to 239 K and it changes sharply below 239 K. The change of photocurrent with temperature is explained in terms of temperature dependence of carrier mobility, lifetime and optical generation rate. Finally, these results will be helpful for precision application of the optoelectronics device in both high and low temperature ambience.

Keywords Si based photodiode · Ideality factor · Tunneling effect · Photocurrent · Optical generation rate · Thermal stress

1 Introduction

For the last several years or so, silicon based photodiodes have played a significant role in different areas of fundamental science as well as in technological applications such as in photometers, sensor for light measuring techniques in cameras, photo-interrupters, IR remote controls and Optically-Coupled Current-Mirror (OCCM) [1–3]. The experimental results of previously published literatures show that photodiodes are extremely temperature sensitive; yet not much work in this direction has been done in the case of commercially available Si photodiodes [1, 4].

The ideality factor (n) and photocurrent (I_{ph}) are such factors which can give important information about the carrier recombination mechanism as well as the opto-electronics performance of the photodiode. We have already undertaken such studies in Si based p-i-n photodiodes that has provided information about the conduction mechanism of this device in the temperature range 350 to 139 K [1]. In our previous work we found that for BPW 21 and BPW 34B photodiodes n increased from 1.07 to 3.56 and 1.02 to 3.71 respectively when the temperature decreased from 350 to 77 K [5]. Characterization of BPW34, Si based photodiode at different temperatures shows that n varies from 1.16 to 2.98 when the temperature is decreased from 300 to 80 K [6].

Temperature dependent photocurrent measurement of a photodiode gives the information of their optical performance at various temperatures which have also an important implication. Xiansong et al. [7] have reported that the photocurrent in green silicon photodiode decreased from approximately 12.6 nA to 9.4 nA when the temperature decreased from 353–213 K. Manik et al. [4] had measured the change of photocurrent in term of photo-voltage (V_{ph}) in TIL-78 photodiode and found that it varied from 50 mV (approx.) to 1900 mV (approx.) when the temperature decreased from room temperature to above liquid nitrogen temperature (we take the data for highest illumination only).

Since the variation of these factors is sensitive to temperature and is also not same for all photodiodes a number

✉ Nabin Baran Manik
nbm_juphysics@yahoo.co.in

[1] Condensed Matter Physics Research Centre, Department of Physics, Jadavpur University, Kolkata, 700 032, India

[2] Present address: Department of Information Engineering, University of Padova, via Gradenigo 6/B, Padova 35131, Italy

of diodes should be characterized so that a theoretical basis of this variation can be addressed. Moreover, such experimental data of commercially available devices over a wide temperature range are not commonly found [4] although various types of photodiodes are available in the market. This article reports the quantitative description of the opto-electronic properties of a typical photodiode VTB8440BH by temperature dependent I–V measurement and photocurrent measurement which will have important implication for low temperature applications. Also, the experimental data obtained in this investigation will be important to design optoelectronic devices involving this photodiode.

2 Experimental Details

In our investigation we used one silicon based p-n photodiode (VTB8440BH) procured from RS Components, having spectral response peak at 580 nm and chip active area is of 5.16 mm^2. Also, their minimum and maximum wavelength detecting capacities are 330–720 nm. The photodiode was placed inside a bath type optical cryostat designed in our laboratory [4].

With special care, liquid nitrogen was poured inside the liquid chamber of the cryostat. The liquid chamber was pre-evacuated to a pressure 10^{-4} Torr by using a high vacuum pumping unit (Model No. PU-2 CH-8, manufactured by Vacuum Products & Consultants) to avoid moisture on the sample. The temperature measurement in the range 350-110 K was executed by using a Chromel-Alumel thermocouple (TC). The TC output was recorded by a Keithley 2000 multimeter with accuracy of the order of ±0.14 K. I–V measurements were performed by using a Keithley 2400 source measure unit.

The photocurrent measurement setup is shown in Fig. 1. In this arrangement the photodiode which was previously placed inside the cryostat is reverse biased with a 2.5 Volt dc source and a 390 KΩ sensing resistance in series. The LED was placed outside the cryostat and driven by a constant current source with a 1 KΩ resistance in series to give a fixed illumination on the photodiode. Due to the incident illumination on photodiode, it generates photocurrent which flows through the sensing resistance and it is measured by a Philips multimeter. The details of the experimental setup are also available in our previous work [8].

3 Results and Discussion

3.1 Forward I-V Characteristics

Typical forward semilog $I - V$ curves are shown in Fig. 2.

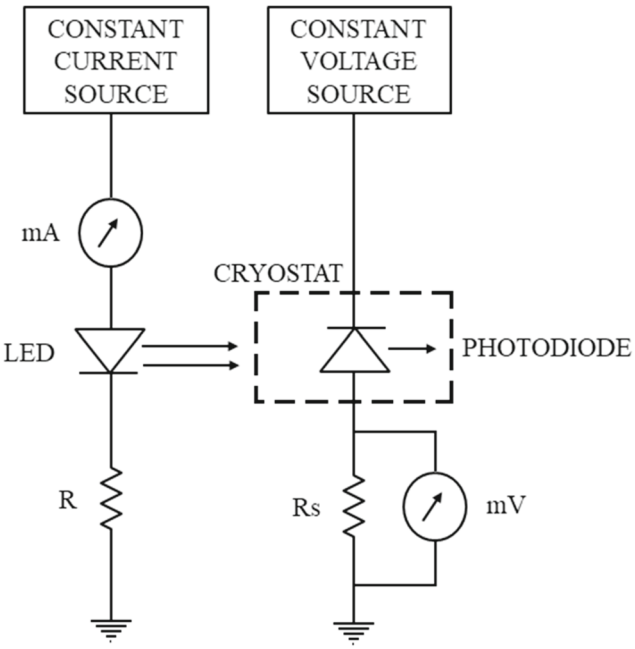

Fig. 1 Schematic diagram of the experimental setup used for the photocurrent measurement

In fact, these curves show distinct three successive linearly dependent segments with different slopes which are dependent on the bias levels. The first segment ($0.4V < V < 0.55V$) is defined as low-bias (I), second segment ($0.55V < V < 0.8V$) as medium-bias (II) and the third one ($0.8V < V < 0.9V$) as the high-bias (III). The leveling of semilog I–V data in region III may be due to space charge limited current and for regions I and II the forward current can be well approximated by the exponential functions [9–11].

$$I_1 = I_{S1}\left[exp\left(qV_j/E_1\right) - 1\right], V_j \geq \quad (1a)$$

$$I_2 = I_{S2}\left[exp\left(qV_j/E_2\right) - 1\right], V_j \geq \quad (1b)$$

where, q is the electron charge, I_{S1}, I_{S2} are the pre-exponential factors, E_1, E_2 are the characteristic energies for low and medium bias level respectively. In general, the I-V characteristics of a $p-n$ junction diode, can be expressed by $I = I_S\exp(qV/nkT–1)$, where K is the Boltzmann constant and T is the temperature. The expected value of n lies between 1 and 2, which strongly implies that the dominant current flows, is mainly diffusion recombination current. But in practice n may increase above 2 with lowering of temperature and it indicates that the tunneling mechanism takes a paramount role in such devices. Apart from tunneling (band to band, via impurity and cascade process) the origin of high ideality factor > 2, has been attributed to carrier leakage [12], multiple diode junctions in a device [13], non-ohmic metal semiconductor contact [14] and partitioning factor of local minority carriers [15]. It is quite

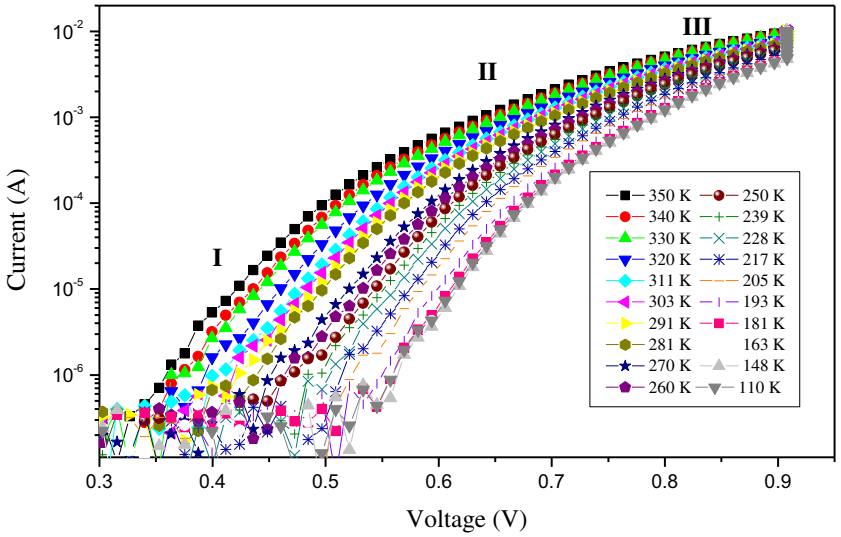

Fig. 2 I-V characteristics of typically VTB8440BH photodiode in the temperature range of 350–110 K

apparent none of the above factors seems to be dominants in the case of photodiode. On the other hand, tunneling seems to be the dominant one because of relatively temperature insensitive characteristics energy (which we would discuss later), an exponential I-V relation together will high value of n.

If we assume the characteristic energies $E_1 = n_1 KT$ for region I and $E_2 = n_2 KT$ for region II, then these energies represent the tunneling transparency of the energy barrier at the junction interface [16]. Hence, it is clear that the characteristic energies are directly proportional to n as well as temperature. Since n is increasing with lowering of temperature, it indicates that the effect of tunneling is gradually increased in lower temperature side and becoming more important at low temperature. The increase of n with lowering of temperature indicates that the defect states within band gap region are increased for decrease the temperature. The increase of ideality factor (>2) the current carriers are tunnel into the available deep-lying defect states in band gap region and recombine non-radiatively. Due to the existing defect sates the tunneling current flow from low current density to high current density of the device through the turn-on of the diode. But the characteristic energy is only slightly dependent on temperature because it is a function of both n and T. The temperature dependence of characteristic energy gives information about the dominant carrier recombination mechanisms. If it depends weakly on temperature, one can interpret that the dominant transport mechanism is associated with tunneling of carriers rather than thermal diffusion. Similar conclusion for different devices has been found by other workers [9] also. The experimental values of ideality factors n_1, n_2 and the characteristic energies E_1, E_2 as obtained from our experimental data are listed in Table 1 and their variations with temperature are shown in Fig. 3.

For an asymmetric step junction, the forward-bias excess current involving deep levels may be written as in the same manner of Eq. 1a, namely, [11]

$$I = I_S \left[exp\left(eV_j/E_T\right) - 1 \right], V_j \geq \tag{2}$$

where E_T is a characteristic energy constant, given by

$$E_T \approx \frac{4eh}{\pi}\left(\sqrt{\frac{N_I}{m_T^* \varepsilon_r \varepsilon_0}}\right) \tag{3}$$

with N_I, the ionized impurity concentration, ε_r, the static dielectric constant, ε_0, the vacuum permittivity and h is Plank's constant. The tunneling effective mass m_T^* is the reduced effective mass of light holes and electrons for an interband (diagonal) tunneling or effective mass of the carriers of one type for band-deep level tunneling.

If we consider the ratio of characteristic energies $E_1/E_2$for both regions, then using Eq. 3 we get $E_1/E_2 = \left(m_{T1}^*/m_{T2}^*\right)^{1/2}$, i.e., the ratio of characteristic energies depends only on the square root of the effective mass of the tunneling entities. So, without knowing the actual value of N_I one can obtain the value of E_1/E_2 by using the values of effective mass of the tunneling entities only. In Si, the effective mass m_T^* for light holes, heavy holes, longitudinal effective mass of electrons and transverse effective mass of electrons are $0.16m_0$, $0.49m_0$, $0.98m_0$ and $0.19m_0$, respectively [17]. The average experimental value of E_1/E_2 in the temperature range 350-193K yields $\sim$ 0.39 which is seen to be approximately consistent with the ratio of the square root of the effective masses for light holes and electrons of Si ($\sim$ 0.403). This consistency between theoretical and experimental values seems to indicate that the tunneling current in low-bias region might be dominated by light holes tunneling via intermediate states while electron tunneling prevails in medium-bias region. It would

Table 1 Experimental values of n_1, n_2, E_1, E_2 (for both low-bias and medium-bias, refer Eq. 1a), E_1/E_2, and V_{ph} at different temperatures

Temperature (K)	n_1	n_2	E_1 (meV)	E_2 (meV)	E_1/E_2	V_{ph} (× 10 mV)
350	1.09	2.76	32.904	83.318	0.395	1.977
340	1.12	2.80	32.844	82.110	0.400	1.977
330	1.16	2.86	33.016	81.403	0.406	1.976
320	1.18	2.91	32.568	80.316	0.406	1.976
311	1.19	2.99	31.920	80.203	0.398	1.976
303	1.21	3.08	31.622	80.492	0.393	1.975
291	1.23	3.18	30.871	79.814	0.387	1.975
281	1.27	3.27	30.780	79.252	0.388	1.975
270	1.33	3.46	30.972	80.575	0.384	1.975
260	1.39	3.64	31.171	81.627	0.382	1.974
250	1.46	3.86	31.481	83.231	0.378	1.974
239	1.52	3.98	31.333	82.043	0.382	1.974
228	1.58	4.21	31.071	82.790	0.375	1.973
217	1.69	4.44	31.630	83.100	0.381	1.972
205	1.82	4.64	32.180	82.041	0.392	1.971
193	1.92	4.87	31.961	81.067	0.394	1.970
181	2.07	5.07	32.315	79.149	0.408	1.969
163	2.24	5.41	31.492	76.058	0.414	1.967
148	2.35	5.71	29.998	72.888	0.412	1.965
110	2.57	6.06	24.383	57.494	0.424	1.962

be better if we explain this result in terms of the energy-wave vector dispersion relation, E-k relation. It is correct that the band diagram, to be precise E-k relation determines the nature of the effective mass through the definition, $m^* \propto (d^2E/dk^2)^{-1}$. Both changes in applied voltage and temperature affect the E-k relation in a significant way. As a result the curvature changes, altering the effective mass. For Si (with existing defect states) the near-band-edge valence-band structure is much more complicated than that of the conduction band. Herein, the top of the valence band which is located at $k = 0$, comprises two distinct bands, designated heavy-hole as well as light-hole bands. Also from our study at present it is not possible to suggest why light hole and electron tunnel at low and medium voltages (see also discussion below).

In the temperature range 181-110 K the value of the ratio is larger than 0.39 and in this temperature range the average experimental value of E_1/E_2 is $\sim$ 0.414. If we replace the light hole mass by the heavy hole mass, the ratio becomes 0.707 even much larger than 0.414. A specific reason for this may be ascribed to the approximate relation that the effective electron mass is proportional to the band gap energy for direct gap crystal [18] but for indirect semiconductor it is generally found that effective mass of both electron and hole are decreased with lowering of temperature [19, 20]. Also it is noted that the rate of change of effective electron mass compared to the effective hole mass with temperature is quite large. In other words we can say the ratio of m^*_{T1}/m^*_{T2} will be increased and may agree with our experimental result. Since temperature dependent effective mass of both carriers for such device is not available then we can't specifically identify that how much it is increased with decrease of temperature. Also we would like to highlight the problem of two bias regions and how the tunneling energy E_1 changes over to E_2 when voltage changes from low to medium. An examination of Eq. 2 implies that this is possible only by a change in the effective mass m* of tunneling carriers, as well other quantities in Eq. 2 remain unchanged for a particular device. The dominant carriers at low and medium bias regions are different. The underlying mechanism is not clear. Two possibilities may be speculated. It may be stated that the defect concentration and distribution as well as structure of the photodiode must have important roles. Another possibility may be that tunneling barriers for light hole and electron are asymmetric [12, 16] and the external electric field may modify the barriers by a different degree so that a current component with a typical tunneling mass may face a favorable barrier. So, the specific device structure, applied electric field and temperature will ultimately decide the nature of tunnel carrier and their variation.

3.2 Temperature Characteristics of Photocurrent

To get the information about the optical properties of the photodiode we measure the photodetector output voltage at

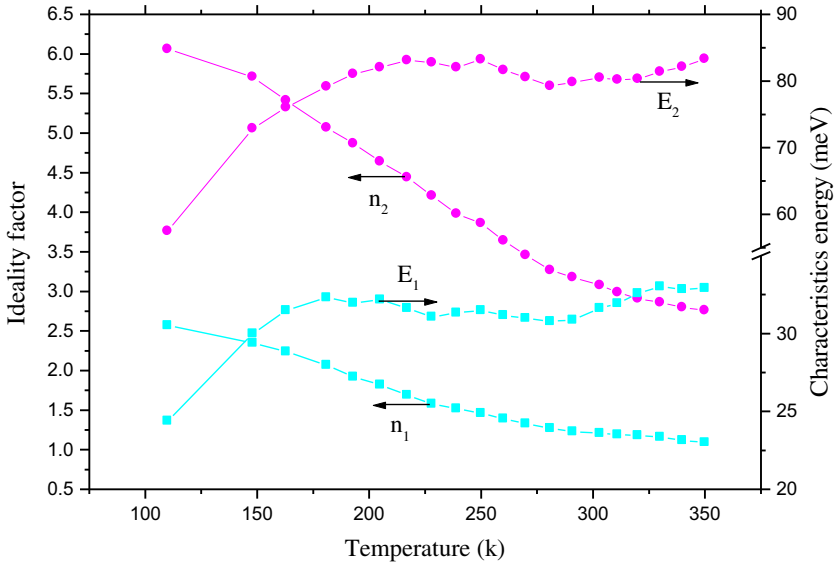

Fig. 3 Variations of characteristic energies (E) and ideality factors (n) as function of temperature. Continuous lines connecting experimental points are only a guide for the eyes

different temperature which is shown in Fig. 4 and tabulated in Table 1.

In order to qualitatively understand the effect of low temperature on the optical characteristics of the photodiode, we consider that when a steady beam of photons is incident on the active region of it then optically generated charge carrier will be concentrated in n- and ptype regions of the photodiode [4]. If we assume the electron hole pairs are produced due to the incident photon only, then the optical generation rate g_{op}, can be written as [21]

$$g_{op} = \frac{\Delta n}{\tau_n}; \quad g_{op} = \frac{\Delta p}{\tau_p} \tag{4}$$

where, Δn, Δp, τ_n and τ_h are the excess charge carrier concentrations and the lifetimes respectively. In such condition the change in photoconductivity will be [21]

$$\Delta\sigma \approx q g_{op} (\tau_n \mu_n + \tau_h \mu_h) \tag{5}$$

where, μ_n and μ_h are the mobilities of electrons and holes respectively. For this device we presume a simple non-radiative recombination which exposes the lifetime of electrons and holes are almost same. Hence, the change of photocurrent with temperature is given by

$$I_{ph} \approx AT^{-2} exp\left(-\frac{E_g}{KT}\right) V \tag{6}$$

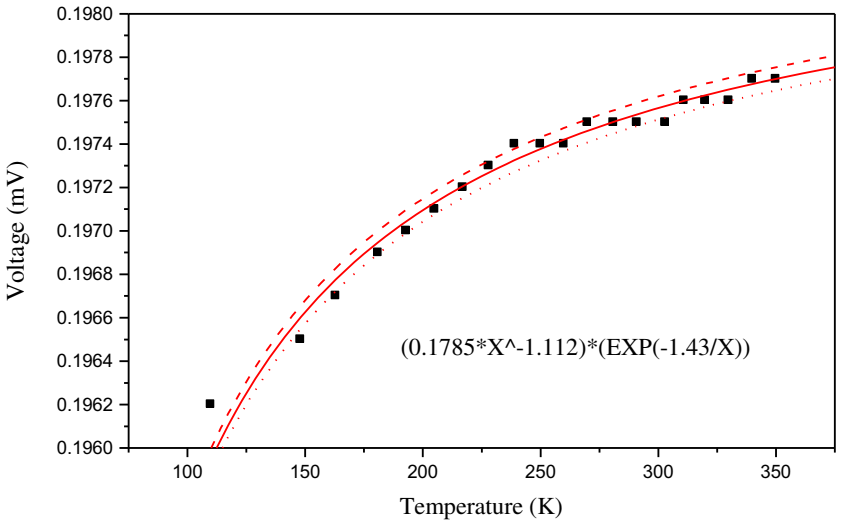

Fig. 4 Variation of the photodiode's output with temperature for fixed illumination incidents on it. Numerical fits, continuous line according to Eq. 6, dash and dot lines indicate the power of the temperature as −1.114 and −1.110 respectively. Again the solid square indicates the experimental points

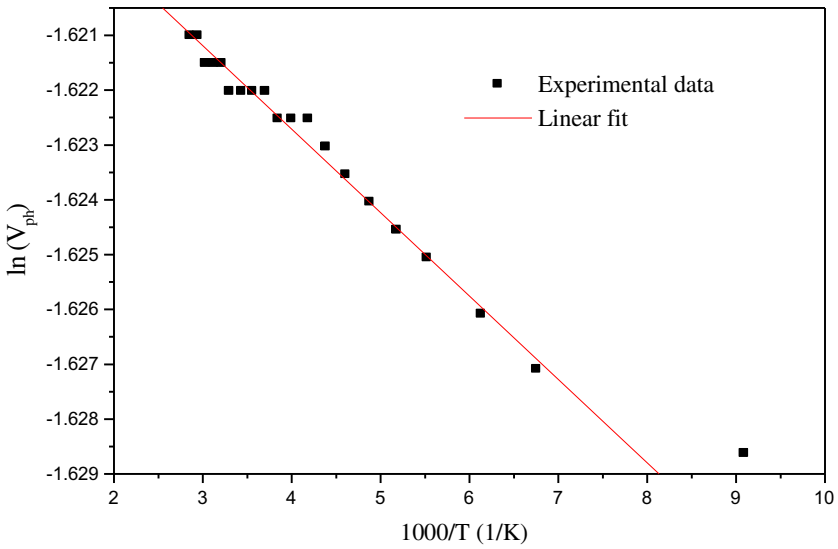

Fig. 5 Plot of $\ln V_{ph}$ versus 1000/T

where, A (= WD/L; W is the chip width, D is the thickness and L is the length) is a temperature independent constant, E_g is the band gap energy of Si and V is the applied voltage across the electrodes. In Eq. 6 it is assumed, $g_{op} \sim \exp(-E_g/KT)$ and the temperature dependence of μ is $T^{-3/2}$, respectively [4]. It is reported that for a package device temperature dependence of τ is very complex and strong temperature dependence is observed at low temperature region rather than high temperature region [5]. Manik et al. [4] assumes temperature dependence of τ is $T^{-3/2}$, whereas our assumption is $T^{-1/2}$. However, to get only the dominant effect, Eq. 6 may be simplified by neglecting the temperature dependence of μ and τ as

$$I_{ph} \sim exp\left(-\frac{\gamma}{T}\right) \tag{7}$$

where, γ is a temperature independent constant. The current according to Eq. 7 is allowed to pass through a sensing resistance R_s. Equation. 6 approximately describes the variation of the photocurrent with temperature. Also, Eq. 7 implies that if we plot $\ln V_{ph}$ versus 1/T curve it should be a straight line. To check the validity of Eq. 7 we plot $\ln V_{ph}$ against 1/T which is shown in Fig. 5 and found that our experimental data qualitatively corroborates with the above relation of photocurrent. Although the curve shows reasonable linearity over a wide range of temperature, a major deviation from linearity at the lower temperature region is also observed. It suggests the exact temperature dependence of μ and τ that is needed to be included in the temperature dependent photocurrent relation especially at low temperature. Since, in Eq. 6 both the temperature dependence of μ and τ is assumed; then finally the experimental data is fitted according to it (see Fig. 4). Form Fig. 4 it is evident that Eq. 6 shows a little improvement at low temperature and the best fit parameters suggest the temperature dependence of τ as $T^{-0.4}$ which supports our assumptions.

4 Conclusions

Our experimental semilog I-V curves exhibit three successive linearly dependent regions along with their bias levels. The variation of ideality factor for both low and medium-bias regions simultaneously increases with the decrease of temperature and it implies that the effect of tunneling is gradually increased in lower temperature side and becomes more important at low temperature. Also, the ratio of characteristic energies E_1/E_2 for low and medium-bias regions suggest that low-bias might be dominated by light holes tunneling via intermediate states while electron tunneling prevails in medium-bias region. The general trend of change of photocurrent is to decrease with lowering of temperature. The experimental results reveal that Eq. 6 explains its temperature dependence. For the present device temperature dependent photocurrent changes according to Eq. 6 rather than Eq. 7 and substantiates our assumptions. These findings of the work are expected to stimulate further theoretical and experimental study to achieve better understanding of the carrier transport mechanisms, the exact nature of carriers and the typical temperature dependence of carrier lifetime in various types of p-n junctions devices.

Acknowledgments The authors acknowledge the Defense Research Development Organization (DRDO), India, for financial assistance, and one of the authors, P. Dalapati is thankful to DRDO for the award of a research fellowship. Also, he has shown his gratitude to M. Mukharjee for giving her support for preparing the manuscript.

References

1. Dalapati P, Manik NB, Basu AN (2014) Influence of temperature on tunneling-enhanced recombination in Si based p–i–n photodiodes. J Semicond 35:082001–082005
2. Camin DV, Valerio G (2006) Cryogenic behavior of optoelectronic devices for the transmission of analog signals via fiber optics. IEEE Trans on Nucl Sci 53:440–443
3. Soref R (2010) Silicon Photonics: A review of recent literature. Silicon 2:1–6
4. Manik NB, Basu AN, Mukherjee SC (2000) Characterisation of the photodetector and light emitting diode at above liquid nitrogen temperature. Cryogenics 40:341–344
5. Dalapati P, Manik NB, Basu AN (2015) Study of effective carrier lifetime and ideality factor of BPW 21 and BPW 34B photodiodes from above room temperature to liquid nitrogen Temperature. Cryogenics 65:10–15
6. Bayhan H, Ozden S (2006) Forward and reverse current–voltage–temperature characteristics of a typical BPW34 photodiode. Solid-State Elect 50:1563–1566
7. Xiansong F, Suying Y, Yunguang Z, Yang Y, Tao G, Maolin D (2010) A study on temperature characteristics of green silicon photodetector . Opt ApplicXL 7597:935–941
8. Dalapati P, Manik NB, Basu AN (2015) Influence of temperature on the performance of high power AlGaInP based red light emitting diode. Opt Quant Electron 47:1227–1238
9. Eliseev PG, Perlin P, Furioli J, Sartori P, Mu J, Osinski M (1997) Tummeling current and electroluminescence in InGaN:Zn, Si/AlGaN/GaN blue light emitting diodes. J Elect Mat 26:311–319
10. Reynolds CL, Patel A (2008) Tunneling entity in different injection regimes of InGaN light emitting diodes. J Appl. Phys 103:086102-1–086102-2
11. Dalapati P, Manik NB, Basu AN (2014) Tunneling current in Si-doped n type-GaAs heterostructures infrared emitter. Front Optoelectron 7:501–508
12. Mayes K, Yasan A, McClintock R, Shiell D, Davish SR, Kung P, Razeghi M (2004) High-power 280 nm AlGaN light-emitting diodes based on an asymmetric single-quantum well. Appl Phys Lett 84:1046–1048
13. Shah JM, Li YL, Gessmann T, Schubert EF (2003) Experimental analysis and theoretical model for anomalously high ideality factors (n>>2.0) in AlGaN/GaN p-n junction diodes. J. Appl Phys 94:2627–2630
14. Zhu D, Xu J, Noemaun AN, Kim JK, Schubert EF, Crawford MH, Koleske DD (2009) The origin of the high diode-ideality factors in GaInN/GaN multiple quantum well light-emitting diodes. Appl Phys Lett 94:081113-1–081113-3
15. Masui H (2011) Diode ideality factor in modern light-emitting diodes. Semicond Sci Technol 26:075011–075016
16. Yan DW, Lu H, Chen DJ, Zhang R, Zheng YD (2010) Forward tunneling current in GaN-based blue light-emitting diodes. Appl Phys Lett 96:083504-1–083504-3
17. Effective mass in semiconductors, http://ecee.colorado.edu/~bart/book/effmass.htm
18. Kittel C (2004) Introduction to solid state physics. 7th ed. Wiley, Singapore, p 214
19. Riffe DM (2002) Temperature dependence of silicon carrier effective masses with application to femtosecond reflectivity measurements. J Opt Soc Am B 19:1092–1100
20. Barber HD (1967) HD. Eeffective mass and intrinsic concentration in silicon. Solid-State Elect 10:1039–1051
21. Nalwa HS (2006) Photodetectors and Fiber Optics:25